New Mexico Geological Society

Downloaded from: https://nmgs.nmt.edu/publications/guidebooks/76



Revisiting the Paleozoic Tectonic and Stratigraphic Evolution of New Mexico Via an 800-km Transect

Kurt Rudolph, Spencer G. Lucas, Sean Connell, Michael Hollerbach, and Crystal Saadeh
2026, pp. 159-174. https://doi.org/10.56577/FFC-76.159

in:

Geology of the Albuquerque Region - Fall Field Conference 2026, Connell, Sean D.; Koning, Daniel J.;, New Mexico Geological Society 76th Annual Fall Field Conference Guidebook, 452 p. https://doi.org/10.56577/FFC-76

This is one of many related papers that were included in the 2026 NMGS Fall Field Conference Guidebook.

Annual NMGS Fall Field Conference Guidebooks

Every fall since 1950, the New Mexico Geological Society (NMGS) has held an annual Fall Field Conference that explores some region of New Mexico (or surrounding states). Always well attended, these conferences provide a guidebook to participants. Besides detailed road logs, the guidebooks contain many well written, edited, and peer-reviewed geoscience papers. These books have set the national standard for geologic guidebooks and are an essential geologic reference for anyone working in or around New Mexico.

Free Downloads

NMGS has decided to make peer-reviewed papers from our Fall Field Conference guidebooks available for free download. This is in keeping with our mission of promoting interest, research, and cooperation regarding geology in New Mexico. However, guidebook sales represent a significant proportion of our operating budget. Therefore, only *research papers* are available for download. *Road logs*, *mini-papers*, and other selected content are available only in print for recent guidebooks.

Copyright Information

Publications of the New Mexico Geological Society, printed and electronic, are protected by the copyright laws of the United States. No material from the NMGS website, or printed and electronic publications, may be reprinted or redistributed without NMGS permission. Contact us for permission to reprint portions of any of our publications.

One printed copy of any materials from the NMGS website or our print and electronic publications may be made for individual use without our permission. Teachers and students may make unlimited copies for educational use. Any other use of these materials requires explicit permission.

This page is intentionally left blank to maintain order of facing pages.

New Mexico Geological Society Guidebook, 76th Fall Field Conference, 2026, p. 159–173, https://doi.org/10.56577/FFC-76.159

REVISITING THE PALEOZOIC TECTONIC AND STRATIGRAPHIC EVOLUTION OF NEW MEXICO VIA AN 800-KM TRANSECT

KURT RUDOLPH[1], SPENCER G. LUCAS[2], SEAN CONNELL[3], MICHAEL HOLLERBACH[4], AND CRYSTAL SAADEH[4]

[1]University of Houston and Rice University, 9 Rabbitbrush, Santa Fe, NM 87506; kwrudolph54@gmail.com
[2]New Mexico Museum of Natural History and Science, 1801 Mountain Road NW, Albuquerque, NM 87104
[3]New Mexico Bureau of Geology and Mineral Resources, 801 Leroy Place, Socorro, NM 87801
[4]TGS, 10451 Clay Road., Houston, TX 77041

Abstract—Using stratigraphic response to infer tectonic elements and evolution, we identify three Paleozoic tectonostratigraphic provinces in New Mexico, documented by a regional stratigraphic cross section, a chronostratigraphic chart, a Pennsylvanian isopach map, basin and flexural models, and outcrop observations. In southeastern New Mexico and west Texas, the Orogrande and greater Permian (Midland and Delaware) basins have a relatively thick, conformable Cambrian to Lower Pennsylvanian ramp succession related to mild extension and sag associated with the Tobosa Basin. This succession is followed by a later (Missourian to Wolfcampian) Ancestral Rocky Mountains (ARM) orogenic event characterized by uplift of the platforms, and rapid basin subsidence. Long-wavelength subsidence took place in Leonardian to Ochoan time, resulting in foundering of both the basins and platforms. In central New Mexico, lower Paleozoic rocks are entirely absent, in an area influenced by the Transcontinental Arch (TCA). The Transcontinental Arch was a low relief, early Paleozoic structural high that bisected the North American continent from Ontario, Canada to New Mexico. Ancestral Rocky Mountains orogenesis commenced earlier than in the southeast, during early Atokan time, as indicated by the onset of rapid subsidence. The Pedernal uplift represents the culmination of the TCA in New Mexico as indicated by the progressive onlap of older Paleozoic strata. Sedimentary rocks as young as Permian rest on Proterozoic basement in the uplift. The thickest Pennsylvanian section is in the Taos–Rainsville trough, where up to 2 km (1.2 mi) of section was deposited in an interpreted flexural basin. To the northwest, the greater Paradox and San Juan basins have thin Cambrian, Devonian, and Mississippian sections. Ancestral Rocky Mountains flexural subsidence, coeval with the emergence of the Uncompahgre uplift, commenced during Atokan time. A thick section of evaporites was deposited in the basin axis. Flexural subsidence continued through the Permian. Forward modeling, tied to isopachs, supports a flexural interpretation for the origin of the Paradox Basin, Orogrande Basin, Delaware Basin, and Taos–Rainsville trough.

INTRODUCTION

The Paleozoic sedimentary succession of New Mexico reflects the tectonic evolution of the region, from an early passive margin to active orogenic deformation. Despite decades of work on individual basins, uplifts, and stratigraphic intervals, an integrated analysis of the spatial and temporal evolution of the Paleozoic in New Mexico remains a challenge.

The purpose of this study is to add to the understanding of the tectonic architecture of Paleozoic New Mexico by examining how major structural elements are represented in the stratigraphic record. We approach this by integrating a regional stratigraphic cross section and accompanying chronostratigraphic chart, a Pennsylvanian isopach map, 1D subsidence (basin) models, and flexural analyses. Together, these tools provide a way to evaluate the magnitude and timing of accommodation changes related to tectonic uplift and subsidence. Our aim is to identify the major structural domains that shaped Paleozoic deposition, determine when they were active, and assess how they interacted to produce the observed stratigraphic architecture. By adding to the understanding of the broader framework, we seek to provide incremental understanding of the regional tectonics, basin evolution, and paleogeography of Paleozoic New Mexico.

GEOLOGIC SETTING

The Paleozoic evolution of New Mexico occurred within a complex tectonic framework shaped by inherited Proterozoic basement structure, early Paleozoic continental-margin dynamics, and late Paleozoic intracontinental deformation. New Mexico's crust consists of 1.65–1.45-Ga juvenile arc and accretionary terranes of the Mazatzal and Picuris orogenic provinces (Karlstrom and Bowring, 1991; Ewing et al., 2019). Many Paleozoic basins and uplifts have been interpreted to have been influenced by this architecture, including the Uncompahgre uplift, Pedernal uplift, Orogrande Basin, and Delaware Basin (Kluth and Coney, 1981).

From the Cambrian to the Devonian, southeast New Mexico occupied a thermally subsiding passive margin that composes the Tobosa Basin (Galley, 1958; Ewing, 2019). Across some of northern and much of central New Mexico, the Transcontinental Arch (TCA) was a low-relief, continent-scale structural high that extended northeast–southwest across the continent. The Transcontinental Arch impacted Cambrian through Mississippian deposition (Sloss, 1988; Carlson, 1999). As a result, the lower Paleozoic succession is either extremely thin or entirely absent across the northeastern and central part of the state, whereas a more complete sedimentary section accumulated in the southeast (Tobosa Basin) and northwest (Paradox region).

Beginning in the Late Mississippian and intensifying during the Pennsylvanian, the southwest Laurentian interior underwent deformation associated with the Ancestral Rocky Mountain (ARM) orogeny, a period of intracratonic, basement-involved deformation (Dickinson et al., 1988; Leary et al., 2017). This was largely driven by the accretion of the Pangean supercontinent (Stevens et al., 2005; Soreghan, et al., 2012; Sweet, et al., 2021). This resulted in the development of paired uplifts and basins across much of the central United States (Fig. 1).

Key ARM features influencing New Mexico during this time include (Fig. 2):

- Uncompahgre uplift and Paradox Basin in the northwest, characterized by rapid flexural subsidence and deposition of thick Pennsylvanian evaporites and Permian alluvial siliciclastic sedimentary rocks (Peterson and Hite, 1969);
- Pedernal uplift and Taos–Rainsville trough in central New Mexico, related to the reactivation of TCA-linked basement highs (Kelley and Silver, 1952; Kottlowski, 1968);
- Orogrande and greater Permian basins and associated uplifts in the southeastern region, which overprinted earlier Tobosa Basin architecture (Pray, 1961; Ewing, 2019).

The ARM orogeny produced strong lateral thickness variations in Pennsylvanian–Wolfcampian successions across the state, with rapidly subsiding basins infilling adjacent to steep-sided, basement-cored uplifts. During the post-Wolfcampian Permian, differential ARM deformation waned, and regional subsidence became more uniform in the southeast (Rudolph, 2023).

METHODS

Stratigraphic Framework

This study constructed and documented a stratigraphic transect across New Mexico from the Permian Basin in the southeast to the Paradox Basin in the northwest.

We utilized both published literature and public domain well data available through the New Mexico and adjoining state websites (Colorado Energy and Carbon Management Commission, 2026; New Mexico Energy, Minerals and Natural Resources Department, 2026; Texas Railroad Commission, 2026; and Utah Department of Natural Resources Division of

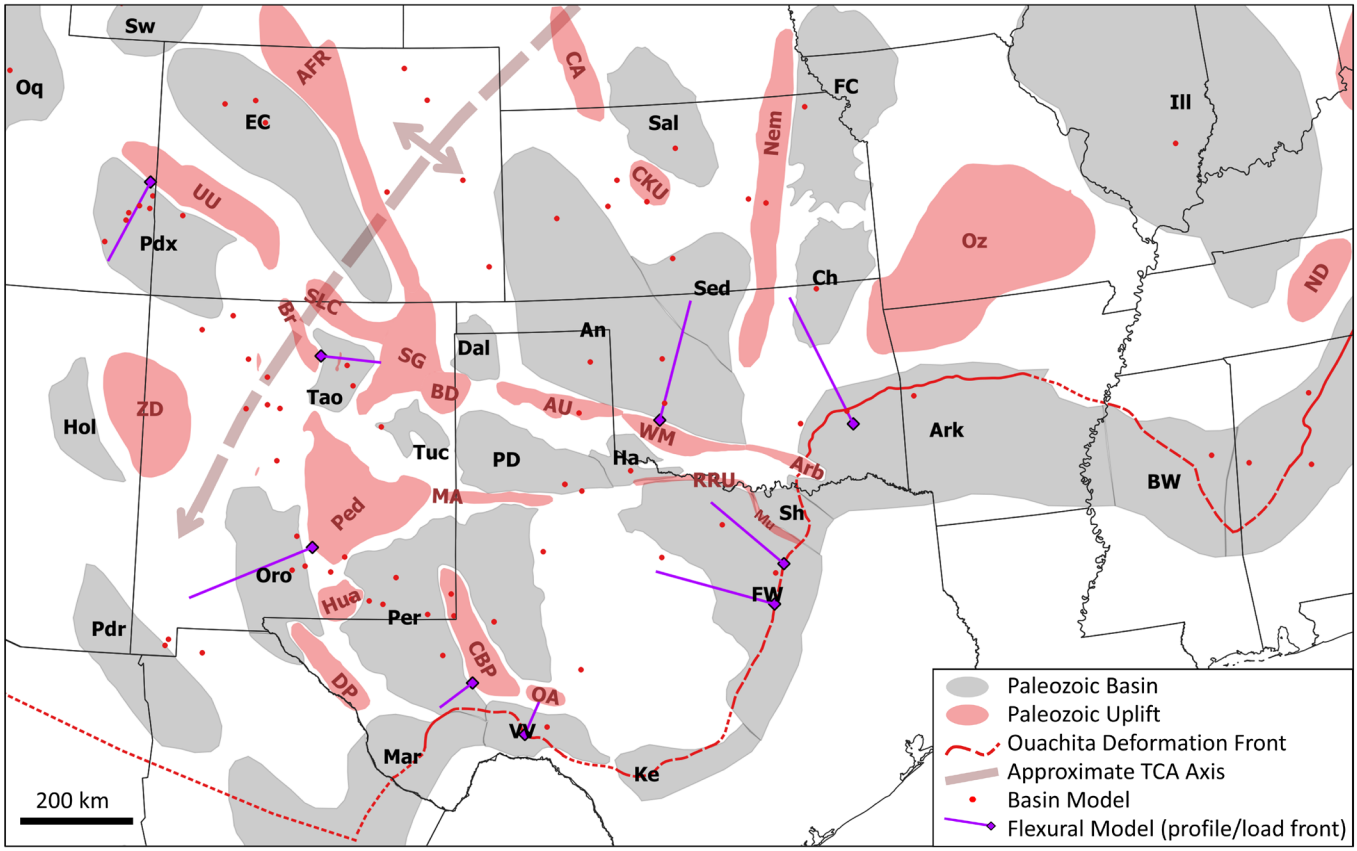


FIGURE 1. Regional map with Paleozoic basins (gray) and ARM uplifts (red), thin-skinned deformation front (red line), axis of TCA (brown dashed line), basin models (red dots), and flexural models (purple lines). Basin outlines are modified from the USGS ArcGIS shapefiles (Coleman and Cahan, 2012). TCA axis is generalized from the mapping of Carlson (1999). Uplift outlines are based and modified from many sources, including original work. Basin abbreviations: An – Anadarko, Ark – Arkoma, BW – Black Warrior, Ch – Cherokee, Dal – Dalhart, EC – Eagle/Colorado, FC – Forest City, Ha – Hardeman, Ill – Illinois, Hol – Holbrook, Ke – Kerr, Mar – Marfa/Marathon, Oq – Oquirrh, Oro – Orogrande, Pdr – Pedregosa, Per – Permian, Pdx – Paradox, Sal – Salina, Sed – Sedgwick, Sh – Sherman, Sw – Sweetwater, Tao – Taos, Tuc – Tucumcari, VV – Val Verde. uplift abbreviations: AFR – Ancestral Front Range, Arb – Arbuckle Mtns., AU – Amarillo uplift, BD – Bravo Dome, Br – Brazos uplift, CA – Cambridge arch, CBP – Central Basin platform, CKU – Central Kansas uplift, DP – Diablo platform, Hua – Huapache uplift, MA – Matador arch, Mu – Muenster arch, Nem – Nemaha uplift, OA – Ozona arch, Oz – Ozark dome, Ped – Pedernal uplift, RRU – Red River uplift, SG – Sierra Grande uplift, SLC – San Luis – Cimarron uplift, UU – Uncompahgre uplift, ZD – Zuni–Defiance uplift.

Oil, Gas and Mining, 2026). The regional cross section X–X' used digital well logs provided courtesy of TGS; these data are proprietary, and only the images are available in this study. Three shorter east–west cross sections (A–A', B–B', C–C') were also constructed, relying mostly on raster logs.

The stratigraphic cross sections (Figs. 3A and 3B; Supplement 1), chronostratigraphic chart (Fig. 4), and basin models (Figs. 4 and 5) rely on both correlated well logs and published measured sections. Biostratigraphically controlled outcrops are the basis of the age model. This includes employment of measured sections from Pray (1961), Armstrong and Mamet (1979), Lucas et al. (1999, 2016a, 2016b, 2021, 2022a, 2022b, in press), and Lucas and Krainer (2024).

Because of uncertainty in the age of sedimentary rocks with a paucity of age-control, diachronous formation tops, and significant regional changes in lithofacies, there is some ambiguity in correlations and age estimates. For example, the Bliss Sandstone of the Permian and Orogrande basins is commonly cited as Cambrian to lowermost Ordovician (Loucks and Kerans, 2019). However, the limited age control in the Franklin Mountains (LeMone, 1969) indicates only Cambrian fauna. The top of the Bliss Sandstone is equated to the top of the Cambrian in this study.

Another important example is the Abo Formation. The top of the Abo is variously estimated as late Wolfcampian to early Leonardian across the study area, likely due to the lithostratigraphic nature of the unit and poor age control (Supplement 1, Table S1.2). The top Abo is the datum on the stratigraphic cross section and is informally designated as "top Wolfcampian" within this study.

The geologic timescale of Gradstein et al. (2020), as implemented in their program Time Scale Creator 8.0, was employed to equate stages to absolute ages (Ma) for input into subsidence analysis.

For the Pennsylvanian isopach in New Mexico (Fig. 2), published mapping studies were employed (e.g., Kottlowski, 1961, 1963; Kottlowski and Havenor, 1962; Roberts et al., 1976; Broadhead and King, 1988; Chowdhury and Sweet, 2020). Data points were digitized in Quantum Geographic Information System software (QGIS) and then manually contoured. Of the 267 control points, most were point estimates from published maps; 62 were new thickness estimates from additional published cross sections and new correlations. These were used as a check on the fidelity of the legacy mapping. Because of the many generations of mapping and various types of data (old logs, modern logs, and measured sections), the accuracy of the information is only fair; thickness errors less than 100 m (328 ft) are expected. Consequently, the contour interval chosen is coarse (0.25 km [820 ft]). For the Paradox and Eagle basins of Utah and Colorado, control points were not available, and the maps of Hart (2021) and Peterson and Hite (1969) were used directly.

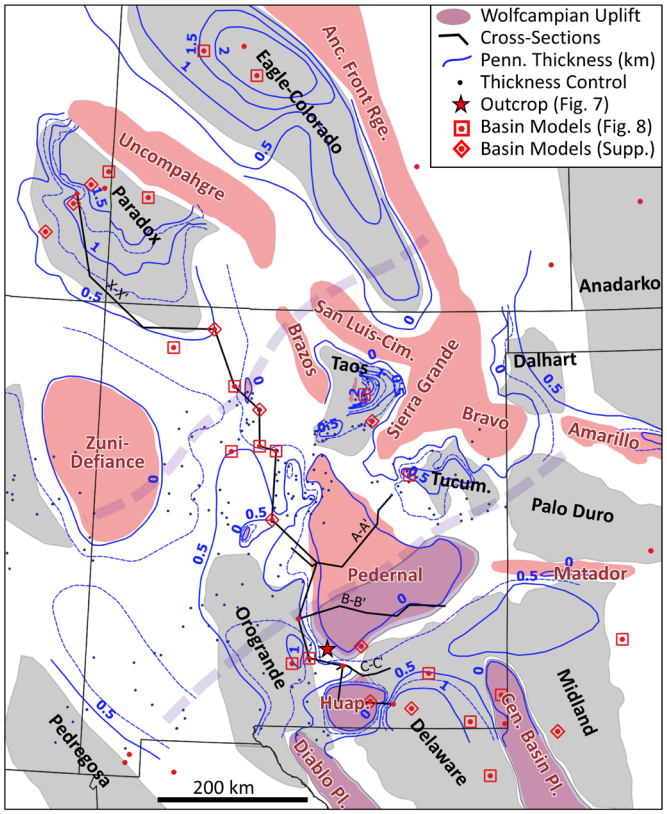


FIGURE 2. Pennsylvanian isopach map in kilometers superimposed on tectonic elements from Figure 1. Contour interval is 0.5 km (0.3 mi; solid) and 0.25 km (0.15 mi; dashed). Also indicated is the location of the regional stratigraphic cross sections, outcrop photo location (star; Fig. 7), and the locations of Wolfcampian uplifts. Three very small positive features are included but not labeled (La Joyita, Peñasco, and El Oro uplifts). The greater Permian Basin is split between the Delaware and Midland basins. The dashed lavender lines approximately subdivide the Paleozoic of New Mexico into three tectonostratigraphic provinces: Southeast, Central and Northwest (refer to text for characteristics). See legend on Figure 1 for legend of other elements.

Basin Models

The Schlumberger application Petromod© was used to construct 1D basin models in the area. The program decompacts (or "backstrips") the section, layer by layer, from the youngest to the oldest horizon. Primary inputs were depths, geologic age, and lithology of the stratigraphic horizons. At each surface, paleobathymetry/paleoelevation, basal heat flow, and paleosurface temperature were also defined. The effect of sediment and water load were also included in the calculations. Erosion of the sedimentary section can also be specified, and whether it was associated with Neogene exhumation or with older unconformities.

Three outputs were generated: depth plots, time plots, and burial-history plots. The parameters of temperature, vitrinite reflectance, porosity, pressure, and thermal conductivity can be displayed in any of these domains. In this study, we only illustrated the burial history. Additional basin model information is included in Supplement 3.

There are two complementary objectives of basin models. First, to evaluate quantitatively the subsidence history. Second, to analyze and predict key parameters over geologic time and depth, especially petroleum-source-rock maturation. The latter application requires a reasonably good understanding of

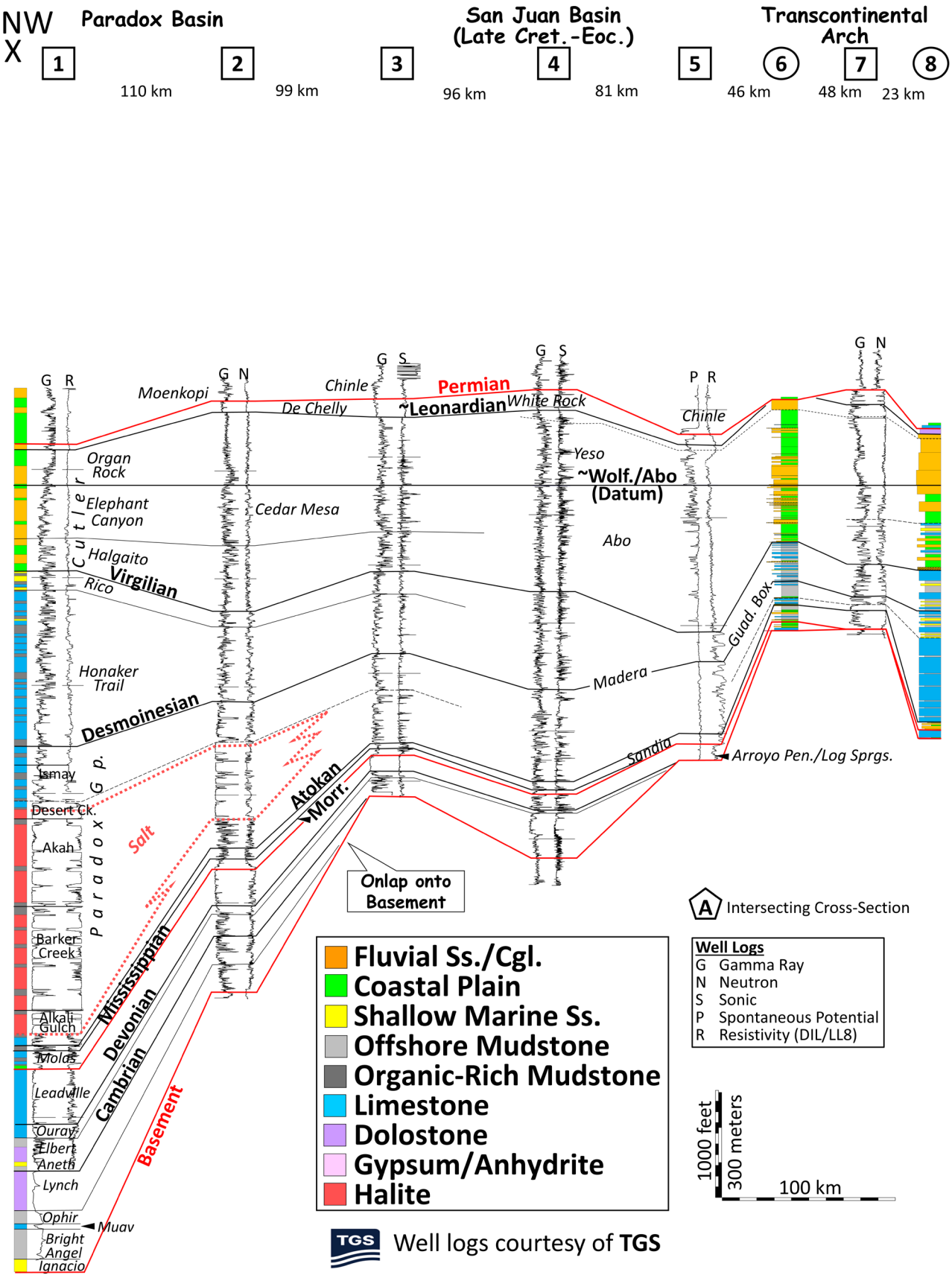
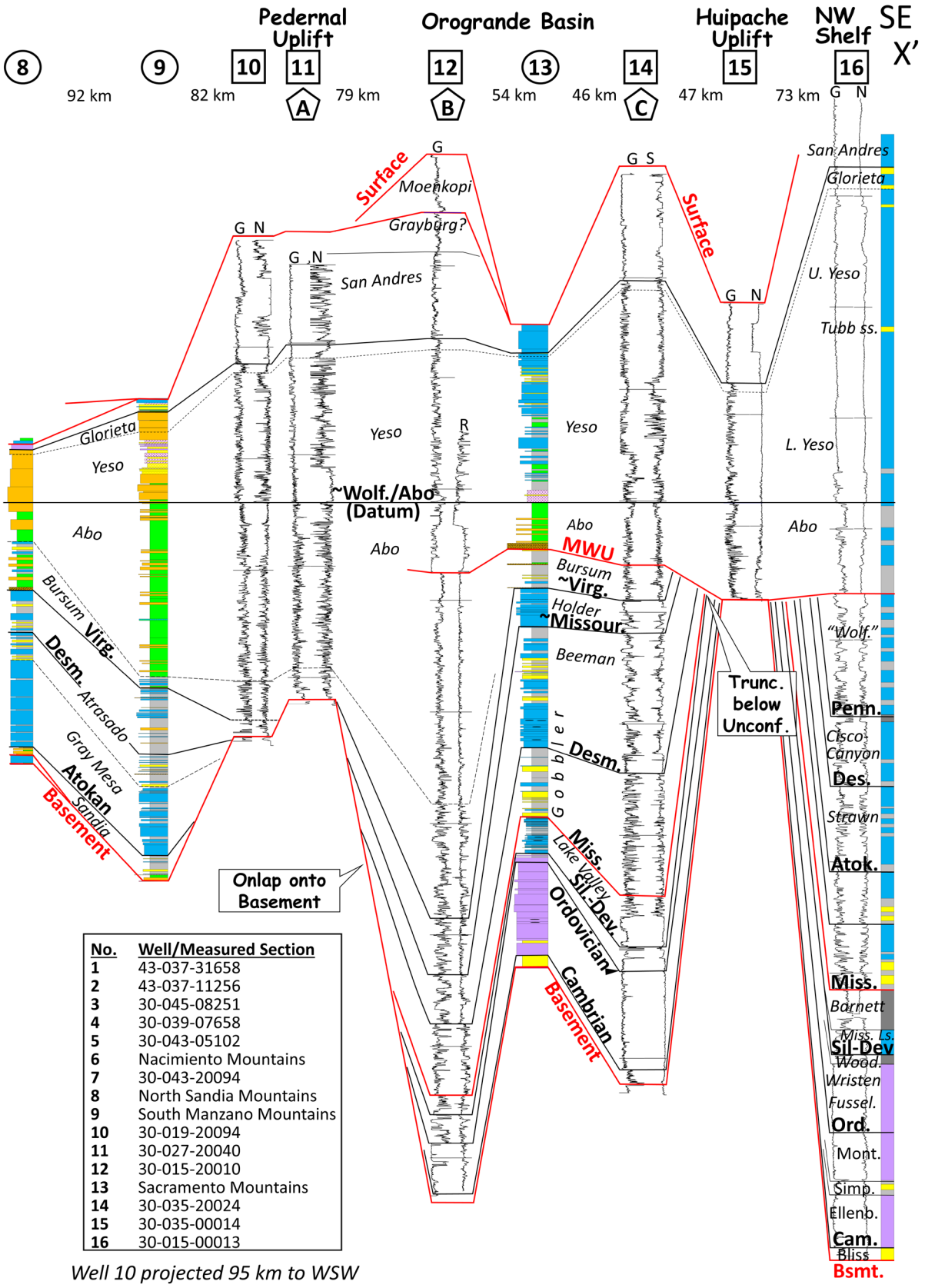


FIGURE 3A. Northwest–southeast stratigraphic cross section X–X', datummed on the top of Abo Formation, or equivalent, in two panels. "MWU" is an abbreviation for the mid-Wolfcampian unconformity. The intersections with cross sections A–A', B–B', and C–C' are indicated. Refer to discussion in text. See Supplement Table S1.1 for the sources of well and measured section control.



No.	Well/Measured Section
1	43-037-31658
2	43-037-11256
3	30-045-08251
4	30-039-07658
5	30-043-05102
6	Nacimiento Mountains
7	30-043-20094
8	North Sandia Mountains
9	South Manzano Mountains
10	30-019-20094
11	30-027-20040
12	30-015-20010
13	Sacramento Mountains
14	30-035-20024
15	30-035-00014
16	30-015-00013

Well 10 projected 95 km to WSW

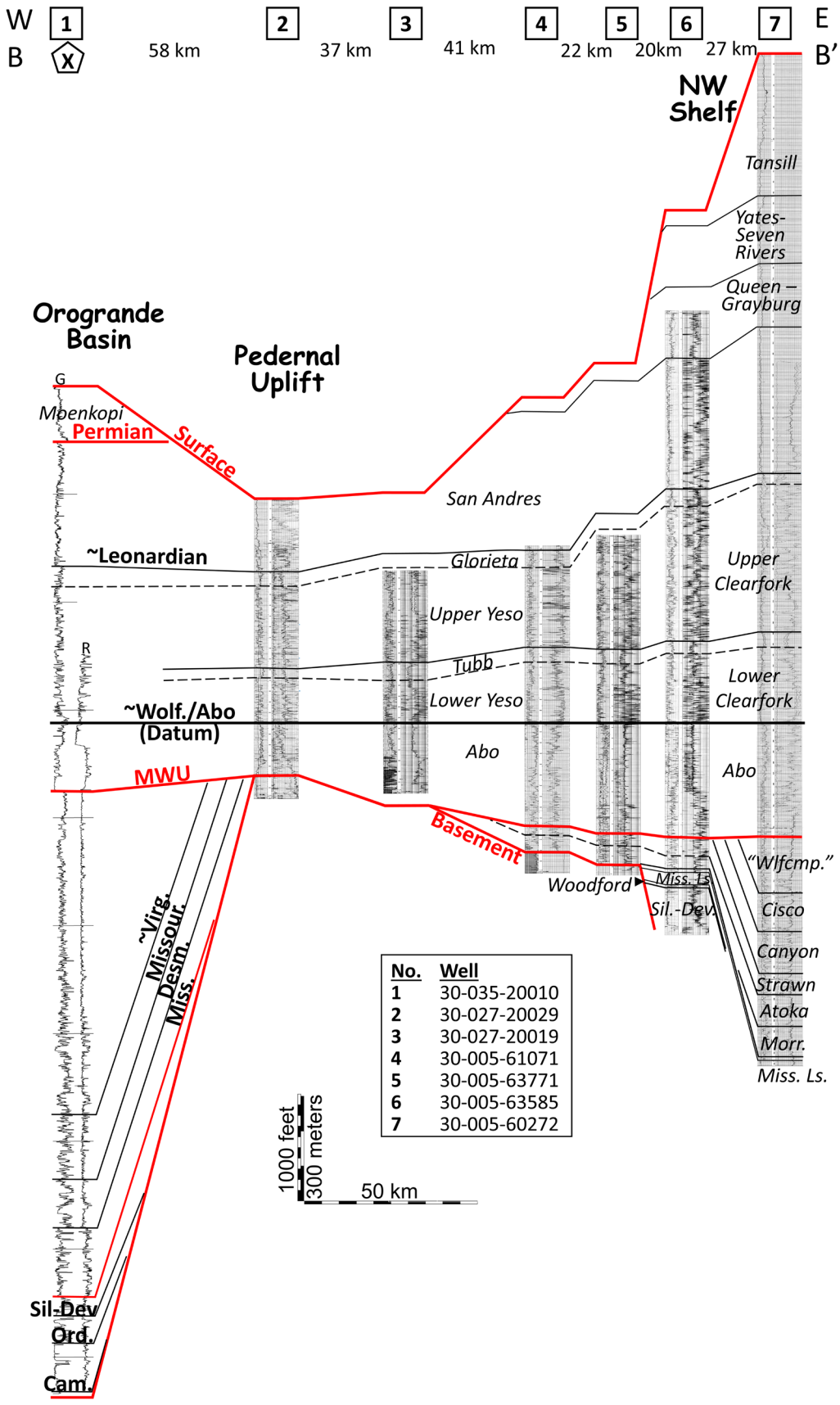


FIGURE 3B. East–west stratigraphic cross section B–B', datummed on the top of the Abo Fm. This transect crosses the southern part of the Pedernal uplift. See Figure 3A for legend. Cross sections A–A' and C–C' are included in Supplement 1.

heat flow history. To test and refine the assumptions on heat flow and burial history, calibrations of model outputs against observed present day temperature and vitrinite reflectance versus depth are important, especially if questions of temperature and/or exhumation history are of interest (Hantschel and Kauerauf, 2009).

A principal objective of this analysis was to understand the subsidence history, so heat flow was generally not as important, and only a few thermal/maturity calibrations were completed. However, in cases where a significant amount of the section of interest has been removed by recent erosion, thermal calibration becomes critical. In this study, basal heat flow was usually interpreted as constant from the Paleozoic to present. An exception was the areas of high modern heat flow associated with the Rio Grande rift system and Jemez Mountains volcanic field. In these instances, heat flow was increased during the Neogene to match the current geothermal gradient using the regional U.S. heat-flow map (Blackwell et al., 2011).

Flexural Modeling

Flexural models for the Paradox Basin, Taos–Rainsville trough, and Orogrande Basin were constructed (procedure described in Saylor et al., 2017). For the Paradox Basin, models were built using isopach maps and a profile of Pennsylvanian and Permian strata from Nuccio and Condon (1996), Condon (1997), Barbeau (2003), and Hart (2021). The Taos–Rainsville trough map was based on Chowdhury and Sweet (2020). The Orogrande model inputs were based on correlations and mapping within this study. The Delaware Basin flexural model employed the lower Wolfcampian isopach map of Fu et al. (2020). The purpose was to test the hypothesis that these three

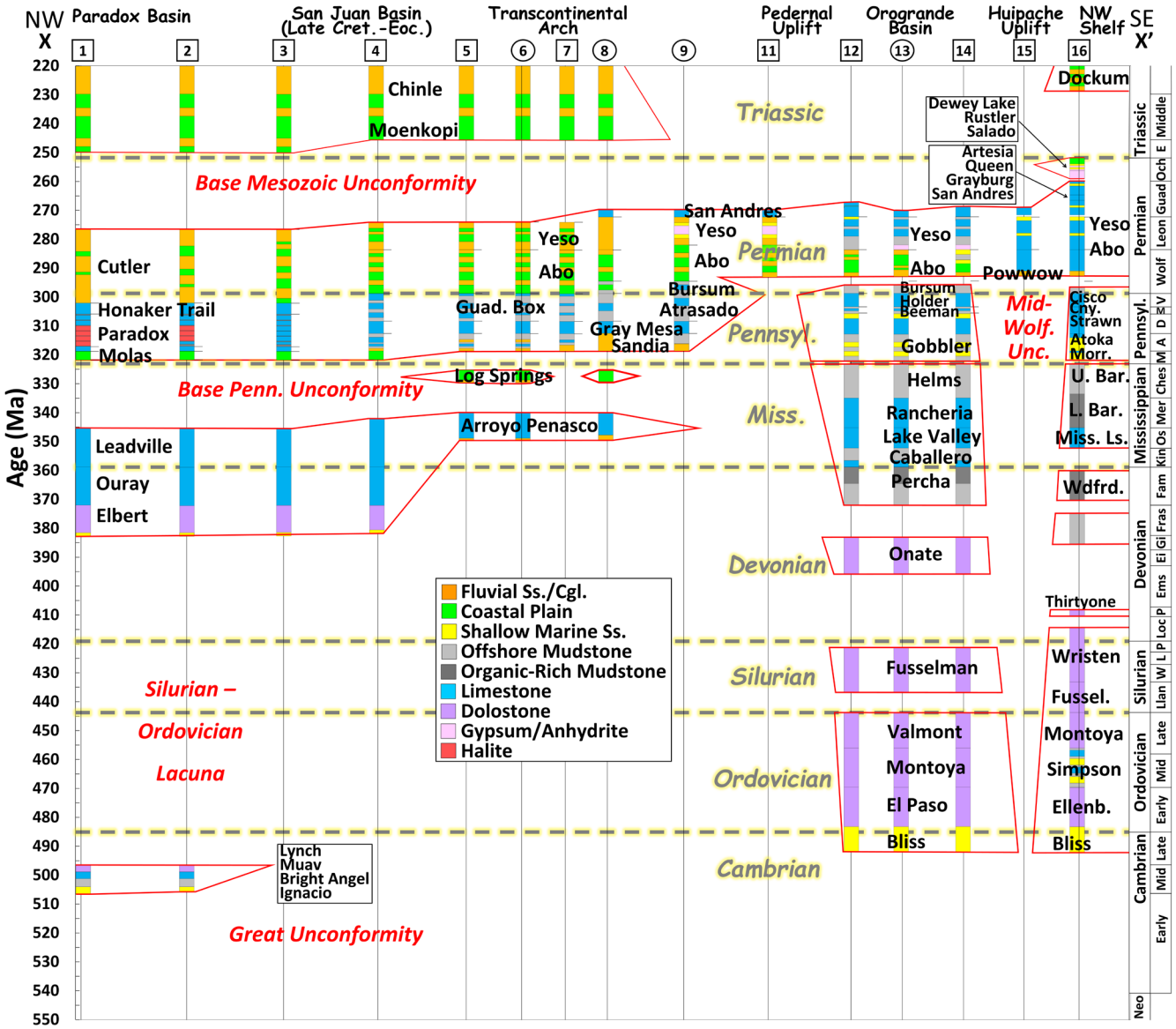


FIGURE 4. Northwest–southeast Paleozoic chronostratigraphic chart, coincident with regional cross section X–X'. See Figure 3 for lithofacies legend.

asymmetric basins are flexural in origin, genetically related to loading by the adjacent ARM uplift.

The primary inputs into the flexural modeling were stratigraphic thickness control points with their position relative to the front of the load. Also specified were the permitted stratigraphic uncertainty/error ranges; acceptable ranges on tectonic load density, front load position, load width and height; and taper direction, maximum slope angle, range of effective elastic thickness (EET) of the coupled lithosphere, and range of load and sediment fill densities. Trials that met the uncertainty criteria were tabulated and reported (means and standard deviations). Models also assumed symmetrical loads, as the uplifts are thick-skinned contractional, basement-involved features. Thus, few assumptions were made about the flexural controls, and the results were observationally driven. Important parameters estimated from modeling were load height, topographic height, load width, slope, and effective elastic thickness. All models assumed an infinite, isotropic plate of uniform thickness. Previous evaluations with a broken plate yielded slightly thicker, but similar EETs (Saylor et al., 2020; Rudolph et al., 2025).

To clarify, effective elastic thickness is a measure of the flexural strength of the coupled lithosphere. High EET yields a broad, but shallow flexure, whereas low EET yields a narrow but deep flexure for the equivalent load (Beaumont, 1981).

RESULTS AND DISCUSSION

The stratigraphic cross sections (Figs. 3A and 3B; Supplement 1) and chronostratigraphic chart (Fig. 4) traverse both uplifts and basins to illustrate the structural architecture across the region. From southeast to northwest, the regional transect X–X' crosses the Northwest shelf of the Permian Basin, the Huapache uplift, the Orogrande Basin, the Pedernal uplift, the central New Mexico area, and the Paradox Basin. The three east–west cross sections further document the morphology of the Huapache and Pedernal uplifts.

We will discuss our observations, first on a spatial basis, dividing the area into three regions: southeast (Orogrande and Permian basins), central (most of New Mexico), and northwest (Paradox and San Juan basins).

Southeast Region

The Permian and Orogrande basins have a similar Paleozoic structural architecture and stratigraphic column, notably a relatively thick and complete succession of pre-Mississippian strata. An upper Cambrian to Lower Ordovician basal transgressive granite wash or sandstone (Bliss) rests on Proterozoic basement. This is followed by a succession of mostly ramp carbonates of Ordovician, Silurian, and Mississippian ages; the Devonian strata are a relatively thin, clastic-dominated stratigraphic interval. In the Permian Basin, there is over a kilometer of pre-Mississippian strata; this thins northward onto the Northwest shelf and into the Orogrande Basin, which has a few hundred meters of lower–middle Paleozoic section.

The maximum early Paleozoic subsidence occurred during the Cambrian–Ordovician, waning into the Devonian (Fig. 5). This has variously been interpreted as a sag basin, with Fairhurst et al. (2021) attributing subsidence to Cambrian rifting followed by thermal sag (Delaware and Oklahoma aulacogens). In particular, the Middle Ordovician Simpson Group thickens to the south (Harrington, 2019; Fairhurst et al., 2021).

The initial onset of ARM subsidence was in the Meramacian (346 Ma; Fig. 6A), but rapid subsidence began in the Missourian (~306 Ma). While the Orogrande, Midland, and Delaware basins were subsiding, the Huapache uplift, Central Basin platform, southern Pedernal uplift, Diablo platform, and Ozona arch were being uplifted (Figs. 2, 3, and 6A; Supplement 3; Ewing, 2019; Zhang et al., 2021). This is evidenced by the progressive subcrop beneath a regional unconformity at or very close to the base of the middle Wolfcampian (Fig. 7; Wahlman, 2019; Fu et al., 2020; Rudolph, 2023; Lucas et al., 2025), and an overlying conglomeratic interval (Powwow Member and more generally, the lower Abo Formation). To clarify, Permian on basement is not evidence of erosion at this mid-Wolfcampian unconformity, as this may have occurred by progressive onlap onto a paleohigh, which may be older; this is the case with the Matador arch and Amarillo uplift in the Texas Panhandle (see well log cross sections of Handford et al., 1981). Well or outcrop control points that indicate subcrop below the unconformity (Wolfcampian on Mississippian to Ordovician) are indicated on Figure 2.

Late Pennsylvanian to Wolfcampian subsidence is consistent with the history of the Val Verde–Marfa foreland basins (Rudolph, 2023). A later docking of Gondwana with Euramerica in the southwest has been attributed to a "zippering" closure from east to west of the megasuture between the two supercontinents (Dickinson and Lawton, 2003).

This subsidence of the subbasins in the Permian Basin is likely flexural, at least in part, with adjacent contractional uplifts loading the lithosphere. This is evidenced by

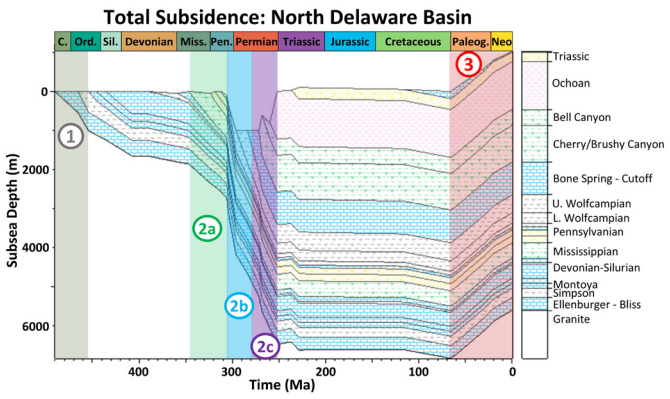


FIGURE 5. Total subsidence curve (Petrel Basin Modeling software) for the Delaware Basin. Three primary subsidence/uplift events are annotated: (1) Early Tobosa rift/sag (Cambrian–Ordovician); (2) ARM subsidence (Late Pennsylvanian to Permian) with three component phases: (a) a late Mississippian to Early Pennsylvanian period of moderate subsidence; (b) a Late Pennsylvanian to early Permian period of differential subsidence of the basins and uplift of the platforms; and (c) a late Permian period of uniform high subsidence of both basins and platforms; and (3) Cenozoic uplift.

wedge-thickening of Wolfcampian strata against the Marathon fold belt for the Val Verde Basin (Rudolph, 2023) and the Central Basin platform for the Delaware Basin. Both examples have been flexurally modelled, and the estimates of flexural rigidity are consistent with modern estimates of EET (Supplement 2).

Detrital zircon provenance studies of the Permian Basin indicate a dominance of Gondwana-derived sediments in the Pennsylvanian–Permian, in response to the Marathon–Ouachita orogeny and Pangea collision/docking (Liu and Stockli, 2019; Soto-Kerans et al., 2020; Waite et al., 2020; Lawton et al., 2021).

The thickest Pennsylvanian section in the Orogrande Basin is on the east flank, adjacent to the Pedernal uplift (Fig. 2). Most of the thickness is in the Upper Pennsylvanian; Missourian to Virgilian (Figure 6A). Flexural modeling was performed to evaluate whether this basin has a flexural component, related to ARM uplift of the southern Pedernal uplift. The result (Fig. 8) indicates that this is tenable, with two points of caution. First, the well and outcrop thickness control is sparse and influenced at its eastern margin by erosion below the mid-Wolfcampian unconformity. Second, the defined wedge is long wavelength, with an implied EET of 53 km (33 mi), compared with modern estimates of about 15 km (9 mi; Supplement Table S2.1; Tesauro et al., 2014).

Saylor et al. (2020) found a similar discrepancy among Cenomanian–Coniacian, Maastrichtian–Eocene, and modern estimates of EET in the Western Interior. Older flexures are longer wavelength with stronger coupled lithosphere implied. They proposed a model in which the Laramide orogeny weakened the crust in that region by hydration and "bulldozing" (thinning at the base) of the overlying slab. In the Orogrande Basin, Cenozoic Basin and Range extension and heating could be an additional factor. However, the ancient (coeval) EET estimate for the Orogrande Basin is higher than other estimates for the western United States

Central Region

The central region area is the southwest extension of the TCA, a long-lived positive feature that influenced early Paleozoic sedimentation (Sloss, 1988; Carlson, 1999). The lower Paleozoic section onlaps basement to the northwest, where no sedimentary rocks older than Mississippian are present over most of northern New Mexico (Carlson, 1999; Figs. 3 and 4). Additionally, the Mississippian (Arroyo Peñasco and Log Springs Formations) is thin (<100 m), or absent (Armstrong and Mamet, 1979). Morrowan-aged rocks have only been identified very locally, in the Jemez Mountains (Osha Canyon Formation; DuChene et al., 1977). Atokan sandstones and shales, with subsidiary limestones, rest on basement in most of the area (e.g., Lucas et al., 2016a).

At least eight uplifts, with thin or absent Pennsylvanian cover, have been identified in the area (e.g., Kottlowski, 1968; Fig. 2). These have rocks as young as Leonardian age resting directly on basement. The largest of these structural features is the Pedernal uplift. While the southern portion shows evidence of subcrop below the mid-Wolfcampian unconformity (MWU), most of the high has no evidence of high amplitude uplifts at that time. Other positive features include the Sierra Grande–Cimarron–Bravo uplifts in northeastern New Mexico, the Brazos uplift in northcentral New Mexico, and the Zuni–Defiance uplift in western New Mexico/eastern Arizona (Fig. 2). Small, discrete uplifts have also been documented, including the La Joyita (Kottlowski and Stewart, 1970), Peñasco (Woodward, 1987), and El Oro–Rincon uplifts (Baltz and Myers, 1999; Chowdhury and Sweet, 2020).

Basin models show an earlier onset of rapid subsidence, relative to the Permian and Orogrande basins (Fig. 5B). There is uncertainty related to the age of the oldest Pennsylvanian strata resting on Mississippian or basement in the basins—generally these rocks are interpreted as Atokan, but they could be as old as Morrowan locally (Taos trough; Baltz and Myers, 1999) or as young as Desmoinesian (Tucumcari Basin; Broadhead and King, 1988). The onset of rapid subsidence was consistently between 320 and 313 Ma. As the youngest sedimentary rocks preserved are early Guadalupian in age (San Andres), the post-Leonardian record is incomplete; therefore, the Guadalupian and Ochoan subsidence relied on reconstruction of eroded section and is uncertain.

The generalized stratigraphic succession can be tied to the tectonic history of the region. The oldest Pennsylvanian strata, the approximately Atokan Sandia Formation, have been characterized as synorogenic mixed carbonate-siliciclastic rocks, comprised of both marine and terrestrial facies. Coarse-grained sandstones and conglomerates are prominent, including basal conglomerates or regoliths (Krainer and Lucas, 2013). The Sandia Formation was deposited at the onset of rapid subsidence, with more subsidence observed in the basins (Taos and Tucumcari) than on the uplifts (Fig. 6B). The younger Desmoinesian to Virgilian strata (formerly Madera Group, now the Gray Mesa and Guadalupe Box/Atrasado Formations) are dominated by marine carbonates, similar to the platform sediments of the Orogrande–Permian basins.

The only thick (>3 km [>1.9 mi]) upper Paleozoic section in central New Mexico is in the Taos–Rainsville trough. A wedge of westerly thickening Pennsylvanian sediments, composed of alluvial/fluvial clastic deposits, with subsidiary shallow marine limestones, occurs in the basin (Casey, 1980; Soegaard, 1990; Baltz and Myers, 1999; Krainer et al., 2004; Chowdhury and Sweet, 2020). Siliciclastic sediments are arkosic and conglomeratic in character, indicative of local sourcing. This, together with the wedge-shaped geometry, is suggestive of a paired ARM uplift and adjacent flexural basin. This idea was evaluated via a flexural model. The favored scenario placed the load front at the Picuris fault (Brazos uplift; Fig. 2) on the west flank. Chowdhury and Sweet (2020) interpreted the El Oro–Rincon uplift as a small emergent feature, lying closer to the west. This was evaluated as an alternative and is in Supplement 2.

For the base case (Brazos uplift), a load of 2.9 km (1.8 mi) with an EET of 14 km (8.7 mi) was modeled (Supplement Table S2.1; Fig. 8). These are reasonable results, and a flexural origin is very likely.

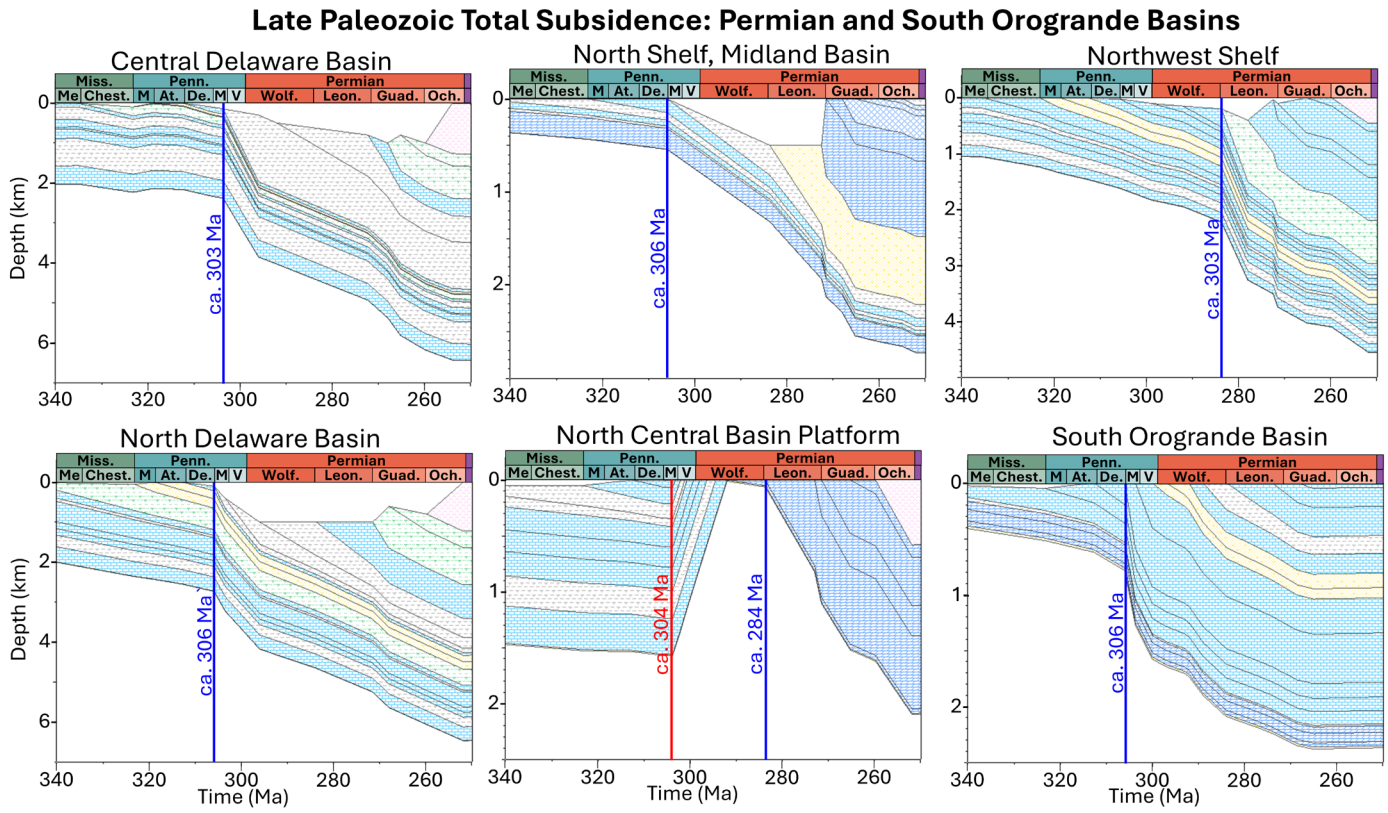


FIGURE 6A. Total subsidence curves for the late Paleozoic from six sites in the southeast area. The onset of rapid subsidence (or uplift) is indicated. Additional models are included in Supplement 3.

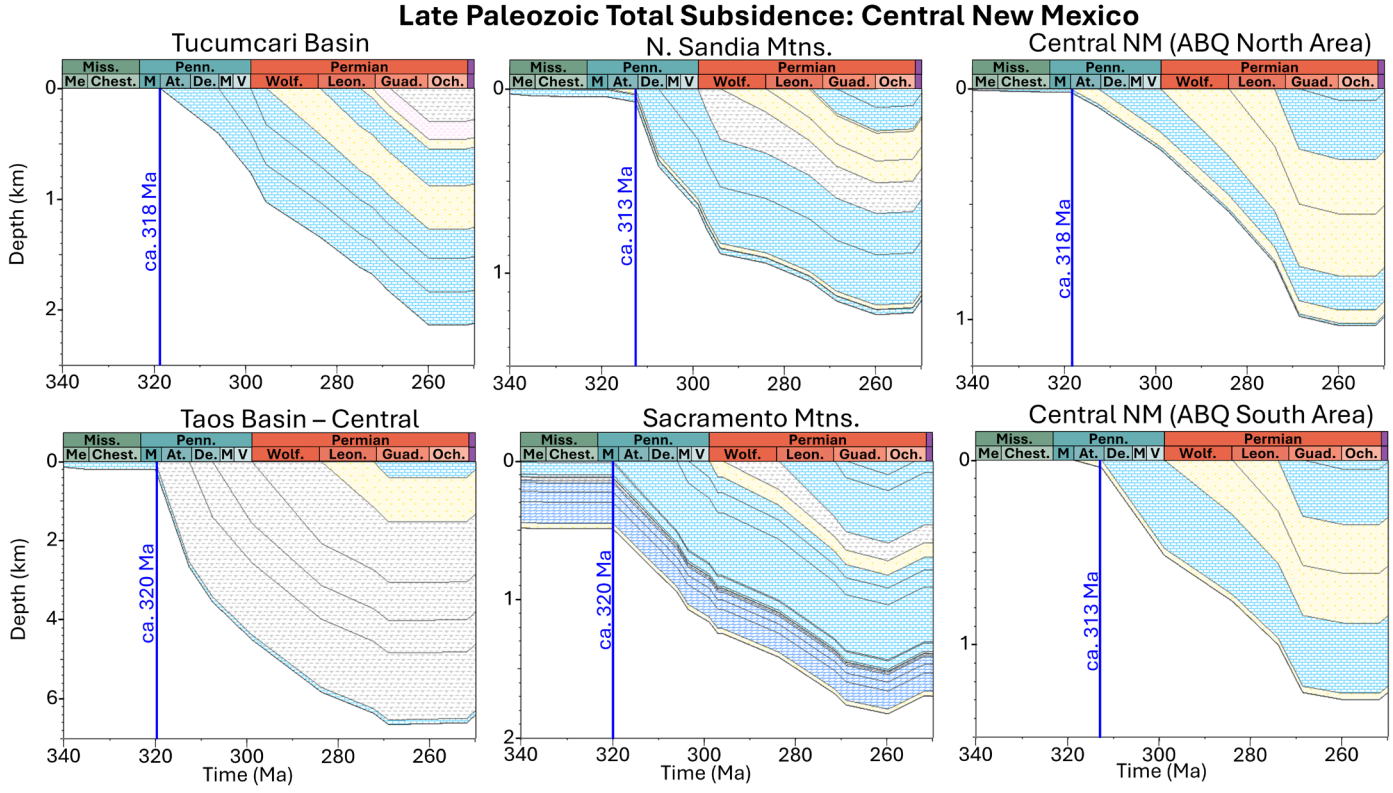


FIGURE 6B. Total subsidence curves for the late Paleozoic from six sites in the central area. The onset of rapid subsidence is indicated. Additional models are included in Supplement 3.

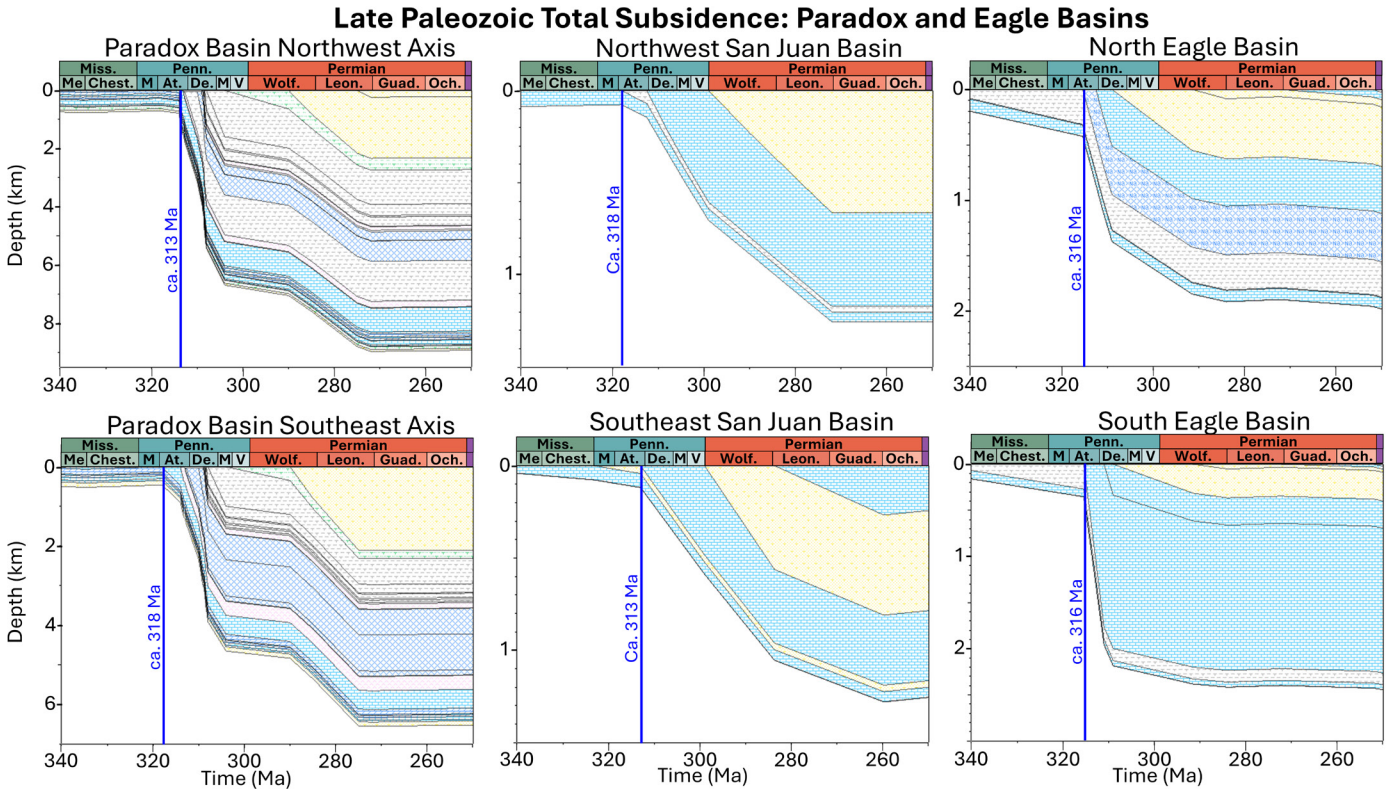


FIGURE 6C. Total subsidence curves for the late Paleozoic from six sites in the northwest area. The onset of rapid subsidence is indicated. Additional models are included in the Supplement 3.

Northwest Region

The northwest region is composed of the Paradox and Eagle basins, separated by the Uncompahgre uplift. To the northwest, pre-Mississippian rocks are present, with a thin Devonian and Cambrian section (Figs. 3 and 4). The Ordovician and Silurian section is absent, but occurs farther west in Utah, where it has been preserved beneath a thick section of Pennsylvanian and Permian in the Oquirrh Basin (Morris and Lovering, 1979). Except for Silurian rocks, a nearly complete lower Paleozoic section is also present in the Sweetwater Basin of southwestern Wyoming (Geldon, 2003). The Paradox Basin shallows towards the southeast into the Late Cretaceous–Paleogene San Juan Basin.

Rapid tectonic subsidence in the Paradox, Eagle, and San Juan basins commenced in middle to late Atokan time, ~ 318–313 Ma (Fig. 5C; Goldhammer et al., 1994; Nucio and Condon, 1996; Rasmussen and Rasmussen, 2009). This succession and series of events were similar to central New Mexico and are consistent with most ARM basins (Sweet et al., 2021). The Pennsylvanian–Permian stratigraphy of the Paradox Basin contains a proximal apron of alluvial fan sediments across the entire stratigraphic interval (Baars and Stevenson, 1981; Luedke and Burbank, 1994). The Pennsylvanian section is dominated by cyclic ramp carbonates and black shales, distal to the uplift (Goldhammer et al., 1994). Additionally, a thick, basin-restricted evaporitic succession (Paradox Formation) dominates the Desmoinesian, with up to a kilometer of halite (excluding highly deformed salt domes). A similar succession, including thick evaporite deposits, also is present in the Eagle Basin of Colorado (Dodge and Bartleson, 1986). Thick evaporites in the Pennsylvanian of Laurentia are not typical and may be related to orographic effects of the ARM and Uncompahgre uplifts (Warren, 2010).

The Cutler Group is composed of terrestrial siliciclastic sedimentary rocks up to 4 km (2.5 mi) thick adjacent to the Uncompahgre uplift. It is mostly Wolfcampian–Leonardian in age but extends into the Late Pennsylvanian in proximal areas (Moore et al., 2008) and it represents the final phase of basin filling and records the termination of rapid subsidence (Fig. 6C).

The Paradox Basin has been previously interpreted as a flexural basin related to the Uncompahgre uplift with a northeasterly thickening wedge of Pennsylvanian to Leonardian strata (e.g., Soreghan et al., 2012). Barbeau (2003) modeled the basin with this premise and proposed a model for a flexural origin based solely on a datummed cross section of the Upper Pennsylvanian interval.

To further validate a flexural origin of the Paradox Basin, four sources of information were modeled: the total Pennsylvanian–Permian (Nucio and Condon, 1996), the Pennsylvanian (Hart, 2021), the Upper Pennsylvanian (Barbeau, 2003), and the somewhat diachronous Upper Pennsylvanian to Permian Cutler Group (Condon, 1997). These are documented in Figure 8 and in Supplement 2. While each scenario has its own uncertainties, the modeling is consistent with a flexural origin of the basin.

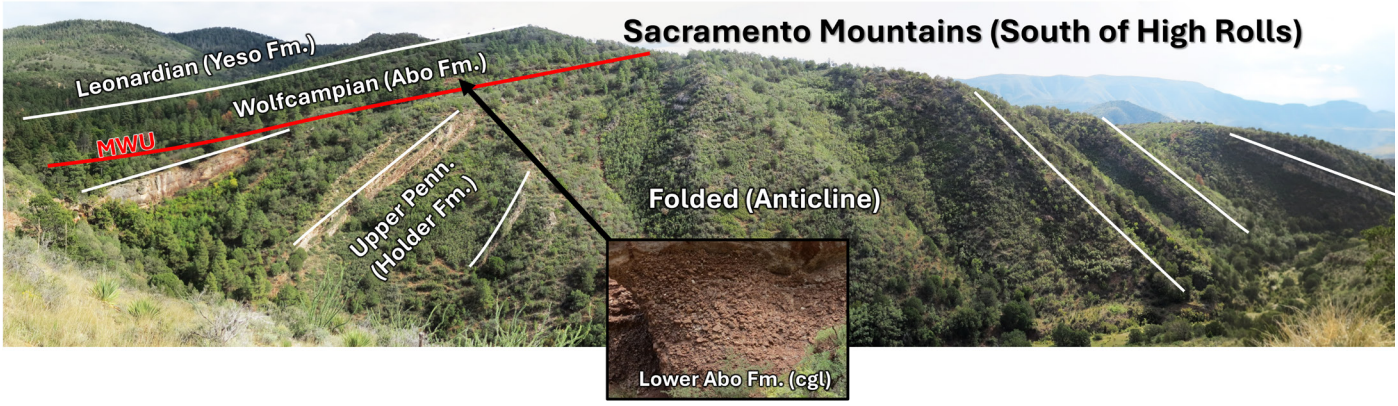


FIGURE 7. Outcrop panorama from south of High Rolls, Sacramento Mountains (looking south, just west of West Side Road [USFS Road 90]). Antiformal Virgilian Holder Formation is truncated below the mid-Wolfcampian unconformity (MWU), with alluvial/fluvial conglomerates of the Wolfcampian Abo Formation immediately above it.

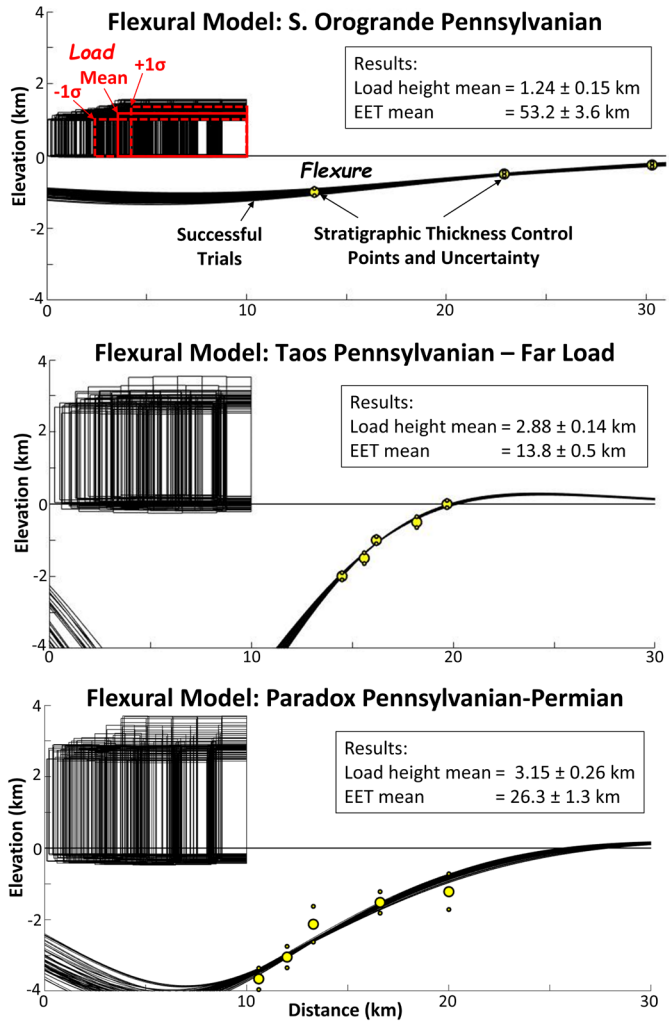


FIGURE 8. Flexural models (Monte Carlo simulation) for the South Orogrande, Taos, and Paradox basins. Additional models are documented in Supplement 3.

Provenance analysis utilizing detrital zircons indicated that Wolfcampian sediments were derived chiefly from the Uncompahgre uplift (Leary et al., 2020). Younger Permian sediments had a more regional source, due to their eolian lithofacies.

CONCLUSIONS

We identify three Paleozoic tectonostratigraphic provinces in New Mexico and adjacent areas based on the stratigraphic response and subsidence analysis: the Permian–Orogrande basins, central New Mexico, and the Paradox–Eagle Basin.

The Permian and Orogrande basins are characterized by a relatively conformable succession of Cambrian through Lower Pennsylvanian strata whose thickness varies gradually. In contrast, the Upper Pennsylvanian to Wolfcampian interval is variable in thickness, with coeval basins and uplifts. There was a major tectonic unconformity in the mid-Wolfcampian related to the ARM orogeny. This is evidenced by progressive subcrop of older strata below the surface, from flanks to crest. Also, a basal fanglomerate (Powwow Conglomerate Member) lies immediately above the unconformity. Rapid subsidence in the basins and concomitant uplift of the platforms commenced at about 306 Ma (Missourian) and possibly included a flexural component. Rapid post-Wolfcampian, subsidence continued but is uniformly distributed over the platforms and basins.

Central New Mexico has no lower Paleozoic sedimentary section, and has Mississippian to Permian rocks resting directly on Proterozoic basement. On the flanks of the TCA, Cambrian through Pennsylvanian sediments progressively onlap positive structural features that include the Pedernal uplift and Sierra Grande arch. We interpret these features as culminations on the greater TCA. Rapid subsidence commenced in central New Mexico in early Atokan time, between 320 and 313 Ma, indicating an earlier onset for the ARM orogeny relative to the greater Permian Basin. The onset of tectonism is marked by a base of Pennsylvanian unconformity, where Atokan-aged strata rest directly on either Mississippian strata or Neoproterozoic basement.

Except for the Taos Trough, the total thickness of the Pennsylvanian–Permian succession in central New Mexico is generally less than 1 km (0.6 mi). In contrast, the time-correlative interval is 1.5–2 km (0.9–1.2 mi) thick in the Orogrande Basin, 2–4 km (1.2–2.5 mi) thick in the Paradox Basin, and 3–5 km (1.9–3.1 mi) thick in the greater Permian Basin. We speculate that the TCA represented a strong and long-lived tectonic

element throughout the Paleozoic, suppressing the local development of deep ARM basins. The Mississippian to Morrowan section is thin or absent with rapid subsidence commencing in the Atokan.

The Paradox Basin contains a thin section of Cambrian, Devonian, and Mississippian rocks. Rapid subsidence commenced in the Atokan, between 318 and 313 Ma, similar to the timing in central New Mexico. Subsidence was flexural, and includes a thick section of Pennsylvanian evaporites and Wolfcampian alluvial fans.

ACKNOWLEDGMENTS

This paper benefited from an early review by Kevin Biddle, and later reviews by Jerry Kendall, Ryan Leary, and Don Yurewicz significantly improved the manuscript. TGS provided digital well logs for the regional cross section (Fig. 3A).

REFERENCES

Armstrong, A.K., and Mamet, B.L., 1979, The Mississippian System of north-central New Mexico: New Mexico Geological Society, Guidebook 30, p. 201–210. https://doi.org/10.56577/FFC-30.201

Baars D.L., and Stevenson, G.M., 1981, Tectonic evolution of the Paradox Basin, Utah and Colorado, *in* Wiegand, D.L., ed., Geology of the Paradox Basin: Denver, Rocky Mountain Association of Geologists, Guidebook, p. 25–31.

Baltz, E.H., and Myers, D.A., 1999, Stratigraphic framework of upper Paleozoic rocks, southeastern Sangre de Cristo Mountains, New Mexico, with a section on speculations and implications for regional interpretation of Ancestral Rocky Mountains paleotectonics: New Mexico Bureau of Mines and Mineral Resources, Memoir 48, 269 p. https://doi.org/10.58799/M-48

Barbeau, D.L., 2003, A flexural model for the Paradox Basin: Implications for the tectonics of the Ancestral Rocky Mountains: Basin Research, v. 15, p. 97–115. https://doi.org/10.1046/j.1365-2117.2003.00194.x

Beaumont, C., 1981, Foreland basins: Geophysical Journal International, v. 65, p. 291–329. https://doi.org/10.1111/j.1365-246X.1981.tb02715.x

Blackwell, D., Richards, M., Frone, Z., Batir, J., Ruzo, A., Dingwall, R., and Williams, M., 2011, Temperature-at-depth maps for the conterminous US and geothermal resource estimates: Southern Methodist University Geothermal Laboratory Geothermal Resources Council Report GRC102945.

Broadhead, R.F., and King, W.E., 1988, Petroleum geology of Pennsylvanian and Lower Permian strata, Tucumcari Basin, east-central New Mexico: New Mexico Bureau of Mines and Mineral Resources, Bulletin 119, 81 p. https://doi.org/10.58799/B-119

Carlson, M.P., 1999, Transcontinental Arch—A pattern formed by rejuvenation of local features across central North America: Tectonophysics, v. 305, p. 225–233. https://doi.org/10.1016/S0040-1951(99)00005-0

Casey, J.M., 1980, Depositional systems and paleogeographic evolution of the Late Paleozoic Taos Trough, northern New Mexico, *in* Fouch, T.D. and Magathan, E.R., eds., Paleozoic Paleogeography of West-Central United States: SEPM Rocky Mountain Section, West-Central United States Paleogeography Symposium, p. 181–196.

Chowdhury, N.U.M.K., and Sweet, D.E., 2020, Subsurface stratigraphy and basin-fill architecture of the late Paleozoic eastern Taos trough, northern New Mexico, U.S.A.: The Mountain Geologist, v. 57, p. 149–176. https://doi.org/10.31582/rmag.mg.57.3.149

Coleman, J.L., Jr., and Cahan, S.M., 2012, Preliminary catalog of the sedimentary basins of the United States: U.S. Geological Survey Open-file Report 2012–1111, 27 p. http://pubs.usgs.gov/of/2012/1111/

Colorado Energy and Carbon Management Commission, 2026, Imaged documents: https://ecmc.colorado.gov/data-maps-reports/imaged-documents (accessed April 2026).

Condon, S.M., 1997, Map of the Paradox Basin and adjacent areas showing thickness of the Pennsylvanian and Permian Cutler Group or Formation: U.S. Geological Survey Bulletin 2000-P, plate 3.

Dickinson, W.R., Klute, M.A., Hayes, M.J., Janecke, S.U., Lundin, E.R., McKittrick, M.A., and Olivares, M.D., 1988, Paleogeographic and paleotectonic setting of Laramide sedimentary basins in the central Rocky Mountain region: Geological Society of America Bulletin, v. 100, p. 1023–1039. https://doi.org/10.1130/0016-7606(1988)100<1023:PAPSOL>2.3.CO;2

Dickinson, W.R., and Lawton, T.F., 2003, Sequential intercontinental suturing as the ultimate control for Pennsylvanian Ancestral Rocky Mountains deformation: Geology, v. 31, p. 609–612. https://doi.org/: 10.1130/0091-7613

Dodge, C.N., and Bartleson, B.L., 1986, The Eagle basin: A new exploration frontier, *in* D.S. Stone, ed., New Interpretations of Northwest Colorado Geology: Denver, Rocky Mountain Association of Geologists, p. 113–122.

DuChene, H., Kues, B.S. and Woodward, L.A., 1977, Osha Canyon Formation (Pennsylvanian), new Morrowan unit in north-central New Mexico: American Association of Petroleum Geologists Bulletin, v. 61, p. 1513–1524. https://doi.org/10.1306/C1EA45C2-16C9-11D7-8645000102C1865D

Ewing, T.E., 2019, Tectonics of the West Texas (Permian Basin)—Origins, structural geology, subsidence, and later modification, *in* Ruppel, S.C., ed., Anatomy of the Paleozoic Basin: The Permian Basin, USA (vol. 1): University of Texas at Austin, Bureau of Economic Geology, Report of Investigations No. 285, p. 63–96. https://doi.org/10.23867/RI0285-1

Ewing, T.E., Barnes, M.A., and Denison, R.E., 2019, Paleozoic foundations of the Permian Basin, west Texas and southeastern New Mexico—A review, *in* Ruppel, S.C., ed., Anatomy of the Paleozoic Basin: The Permian Basin, USA (vol. 1): University of Texas at Austin, Bureau of Economic Geology, Report of Investigations No. 285, p. 43–61. https://doi.org/10.23867/RI0285-1

Fairhurst, B., Ewing, T., and Lindsay, B., 2021, West Texas (Permian) Super Basin, United States: Tectonics, structural development, sedimentation, petroleum systems, and hydrocarbon reserves: American Association of Petroleum Geologists Bulletin, v. 105, p. 1099–1147. https://doi.org/10.1306/03042120130

Fu, Q., Baumgardner, R.W., Jr., and Hamlin, H.S., 2020, Early Permian (Wolfcampian) succession in the Permian Basin: Icehouse platform, slope carbonates, and basinal mudrocks, *in* Ruppel, S. C., ed., Anatomy of a Paleozoic Basin: The Permian Basin, USA (vol. 2): University of Texas at Austin, Bureau of Economic Geology, Report of Investigations No. 285, p. 185–226. https://doi.org/10.23867/RI0285-2, p. 185–226

Galley, J.E., 1958, Oil and geology in the Permian Basin of Texas and New Mexico, *in* Weeks, L.G., ed., Habitat of Oil: Tulsa, American Association of Petroleum Geologists, p. 395–446.

Geldon, A.L., 2003, Geology of Paleozoic rocks in the Upper Colorado River Basin in Arizona, Colorado, New Mexico, Utah, and Wyoming, excluding the San Juan Basin: U.S. Geological Survey Professional Paper 1411-A, 85 p. https://doi.org/10.3133/pp1411A

Goldhammer, R.K., Oswald, E.J., and Dunn, P.A., 1994, High-frequency, glacio-eustatic cyclicity in the Middle Pennsylvanian of the Paradox Basin, *in* De, B.P.L. and Smith, D.G., eds., Orbital Forcing and Cyclic Sequences: Special Publication International Association of Sedimentologists, v. 19, p. 243–283. https://doi.org/10.1002/9781444304039.ch18

Gradstein, F.G., Ogg, J.G., Schmitz, M.D., and Ogg, G.M., eds., 2020, Geologic Time Scale 2020: Amsterdam, Elsevier, 240 p. https://doi.org/10.1127/nos/2020/0634

Handford, C.R., Dutton, S.P., and Fredericks, P.E., 1981, Regional cross sections of the Texas Panhandle: Precambrian to mid-Permian: The University of Texas at Austin, Bureau of Economic Geology, 8 p., 7 plates.

Hantschel, T., and Kauerauf, A.I., 2009, Fundamentals of Basin and Petroleum Systems Modeling: Berlin, Springer-Verlag, 476 p. https://doi.org/10.1007/978-3-540-72318-9

Harrington, R.R., 2019, The Middle–Upper Ordovician Simpson Group of the Permian Basin: Stratigraphy, lithofacies, and reservoir development, *in* Ruppel, S.C., ed., Anatomy of a Paleozoic Basin: The Permian Basin, USA (vol. 1): University of Texas at Austin, Bureau of Economic Geology, Report of Investigations No. 285, p. 331–352. https://doi.org/10.23867/RI0285-1

Hart, B.S., 2021, Stratigraphy and hydrocarbon resources of the San Juan Basin: Lessons for other basins, lessons from other basins: The Mountain Geologist, v. 58, p. 43–103. https://doi.org/10.31582/rmag.mg.58.2.43

Karlstrom, K.E., and Bowring, S.A., 1991, Early Proterozoic assembly of tectonostratigraphic terranes in southwestern North America: The Journal of Geology, v. 96, no. 5, p. 561–576. https://doi.org/10.1086/629252

Kelley, V. C., and Silver, C., 1952, Geology of the Caballo Mountains: University of New Mexico, Publications in Geology, no. 4, 286 p.

Kluth, C.F., and Coney, P.J., 1981, Plate-tectonics of the Ancestral Rocky Mountains: Geology, v. 9, no. 1, p. 10–15. https://doi.org/10.1130/0091-7613(1981)9<10:PTOTAR>2.0.CO;2

Kottlowski, F.E., 1961, Pennsylvanian rocks in north-central New Mexico: New Mexico Geological Society, Guidebook 12, p. 97–104. https://doi.org/10.56577/FFC-12.97

Kottlowski F.E., 1963, Paleozoic and Mesozoic strata of southwestern and south-central New Mexico: New Mexico Bureau of Mines and Mineral Resources, Bulletin 79, 100 p. https://doi.org/10.58799/B-79

Kottlowski, F.E., 1968, Influence of the Pedernal uplift on sedimentation: Basins of the Southwest: North Texas Geological Society and West Texas Geological Society, v. 1, p. 21–40.

Kottlowski, F.E., and Havenor, K.C., 1962, Pennsylvanian rocks of the Mogollon Rim area, Arizona: New Mexico Geological Society, Guidebook 13, p. 77–83. https://doi.org/10.56577/FFC-13.77

Kottlowski, F.E., and Stewart, W.J., 1970, Part I—The Wolfcampian Joyita uplift in Central New Mexico: New Mexico Bureau of Geology and Mineral Resources, Memoir 23, p. 1–31.

Krainer, K., and Lucas, S.G., 2013, The Pennsylvanian Sandia Formation in northern and central New Mexico, *in* Lucas, S.G., Nelson, W.J., DiMichele, W.A., Speilmann, J.A., Krainer, K., Barrick, J.E., Elrick, S., and Voigt, S., eds., Carboniferous-Permian Transition in Central New Mexico: New Mexico Museum of Natural History and Science, Bulletin 59, p. 77–100. https://doi.org/10.56577/SM-2013.32

Krainer, K., Lucas, S.G., and Kues, B.S., 2004, Tectonically induced clastic carbonate depositional sequences of the Pennsylvanian–Permian transition in the Rowe-Mora basin, northern New Mexico: New Mexico Geological Society, Guidebook 55, p. 314–325. https://doi.org/10.56577/FFC-55.314

Lawton, T.F., Blakey, R.C., Stockli, D.F., and Liu, L., 2021, Late Paleozoic (Late Mississippian–Middle Permian) sediment provenance and dispersal in western equatorial Pangea: Palaeogeography, Palaeoclimatology, Palaeoecology, v. 572, p. 1–35. https://doi.org/10.1016/j.palaeo.2021.110386

Leary, R.J., Umhoefer, P., Smith, M.E., and Riggs, N., 2017, A three-sided orogen: A new tectonic model for Ancestral Rocky Mountain uplift and basin development: Geology, v. 45, p. 735–738. https://doi.org/10.1130/G39041.1

Leary, R.J., Umhoefer, P., Smith, M.E., Smith, T.M., Saylor, J.E., Riggs, N., Burr, G., Lodes, E., Foley, D., Licht, A., Mueller, M.A., and Baird, C., 2020, Provenance of Pennsylvanian–Permian sedimentary rocks associated with the Ancestral Rocky Mountains orogeny in southwestern Laurentia: Implications for continental-scale Laurentian sediment transport systems: Lithosphere, v. 12, p. 88–121. https://doi.org/10.1130/L1115.1

LeMone, D., 1969, Lower Paleozoic rocks in the El Paso area: New Mexico Geological Society, Guidebook 20, p. 68–79. https://doi.org/10.56577/FFC-20.68

Liu, L., and Stockli, D.F., 2020, U-Pb ages of detrital zircons in lower Permian sandstone and siltstone of the Permian Basin, west Texas, USA: Evidence of dominant Gondwanan and peri-Gondwanan sediment input to Laurentia: Geological Society of America Bulletin, v. 132, p. 245–262. https://doi.org/10.1130/B35119

Loucks, R.G., and Kerans, C., 2019, Geologic review of the Lower Ordovician Ellenburger Group of the Permian Basin, west Texas and southeast New Mexico, *in* S. C. Ruppel, ed., Anatomy of a Paleozoic Basin: The Permian Basin, USA (vol. 1): University of Texas at Austin, Bureau of Economic Geology, Report of Investigations No. 285, p. 295–330. https://doi.org/10.23867/RI0285-1

Lucas, S.G., Rowland, J.M., Kues, B.S., Estep, J.W., and Wilde, G.L., 1999, Uppermost Pennsylvanian and Permian stratigraphy and biostratigraphy at Placitas, New Mexico: New Mexico Geological Society, Guidebook 50, p. 281–292. https://doi.org/10.56577/FFC-50.281

Lucas, S.G., Krainer, K., Oviatt, C.G., Vachard, D., Berman, D.S., and Henrici, A.C., 2016a, The Permian system at Abo Pass, central New Mexico (USA): New Mexico Geological Society, Guidebook 67, p. 313–350. https://doi.org/10.56577/FFC-67.313

Lucas, S.G., Krainer, K., and Vachard, D., 2016b, The Pennsylvanian section at Priest Canyon, southern Manzano Mountains, New Mexico: New Mexico Geological Society, Guidebook 67, p. 275–301. https://doi.org/10.56577/FFC-67.275

Lucas, S.G., DiMichele, W.A., Krainer, K., Barrick, J.E., Vachard, D., Donovan, M.P., Looy, C., Kerp, H., and Chaney, D.S., 2021, The Pennsylvanian System in the Sacramento Mountains, New Mexico, USA: Smithsonian Contributions To Paleobiology, Number 104, 215 p. https://doi.org/10.5479/si.14079809.v1

Lucas, S.G., Krainer, K., and Barrick, J.E., 2022a, Pennsylvanian stratigraphy and biostratigraphy in the Cerros de Amado, Socorro County, New Mexico: New Mexico Geological Society, Guidebook 72, p. 147–164. https://doi.org/10.56577/FFC-72.147

Lucas, S.G., Krainer, K., and Nelson, W.J., 2022b, Permian stratigraphy east of Socorro, central New Mexico: New Mexico Geological Society, Guidebook 72, p. 187–201. https://doi.org/10.56577/FFC-72.187

Lucas, S.G., and Krainer, K., 2024, Upper Paleozoic stratigraphy around the Sierra Nacimiento, San Pedro Mountains, and Jemez Mountains, northern New Mexico: New Mexico Geological Society, Guidebook 74, p. 141–156. https://doi.org/10.56577/FFC-74.141

Lucas, S.G., Krainer, K., and Le Coze, F., 2025, The lower Permian Hueco Group and Abo Formation in southern New Mexico and Hueco Group correlations in New Mexico-west Texas: New Mexico Museum of Natural History and Science, Bulletin 101, p. 188–259.

Lucas, S.G., Krainer, K., DiMichele, W.A., Allen, B.D., Barrick, J.E., Vachard, D., Eble, C., Bashforth, A.R., Donovan, M.P., Ernst, A., Pfefferkorn, H.W., and May, P.T., in press, The Pennsylvanian System in the Sandia Mountains, New Mexico, USA: Stratigraphy, petrography, paleontology, depositional systems, biostratigraphy, and geologic history: Smithsonian Contributions to Paleobiology.

Luedke, R.G., and Burbank, W.S., 1994, Measured stratigraphic sections in the Ouray area, western San Juan Mountains, Colorado: U.S. Geological Survey Open-File Report 94-583, 28 p. https://doi.org/10.3133/ofr94583

Moore, K.D., Soreghan, G.S., Sweet, D.E., 2008, Stratigraphic and structural relations in the proximal Cutler Formation of the Paradox Basin: Implications for timing of movement on the Uncompahgre Front: The Mountain Geologist, v. 45, p. 49–68.

Morris, H.T., and Lovering, T.S., 1979, General geology and mines of the East Tintic Mining District, Utah and Juab counties, Utah: U.S. Geological Survey Professional Paper 1024, 203 p.

New Mexico Energy, Minerals and Natural Resources Department, 2026, OCD data: https://www.emnrd.nm.gov/ocd/ocd-data/ (accessed April 2026).

Nuccio, V.F., and Condon, S.M., 1996, Burial and thermal history of the Paradox Basin, Utah and Colorado, and petroleum potential of the Middle Pennsylvanian Paradox Formation: U.S. Geological Survey Bulletin 2000–O, 41 p., 2 plates.

Peterson, J.A., and Hite, R.J., 1969, Pennsylvanian evaporite-carbonate cycles and their relation to petroleum occurrence, Southern Rocky Mountains: The American Association of Petroleum Geologists Bulletin, v. 53, p. 884–908. https://doi.org/10.1306/5D25C807-16C1-11D7-8645000102C1865D

Pray, L.C., 1961, Geology of the Sacramento Mountains escarpment, Otero County, New Mexico: New Mexico Bureau of Mines and Mineral Resources, Bulletin 35, 144 p. https://doi.org/10.58799/B-35

Rasmussen, L., and Rasmussen, D.L., 2009, Burial history analysis of the Pennsylvanian petroleum system in the deep Paradox Basin Fold and Fault Belt, Colorado and Utah, *in* Houston, W.S., Wray, L.L., and Moreland, P.G., eds., The Paradox Basin Revisited—New Developments in Petroleum Systems and Basin Analysis: Rocky Mountain Association of Geologists Special Publication, p. 24–94.

Roberts, J.W., Barnes, J.J., and Wacker, H.J., 1976, Subsurface Paleozoic stratigraphy of the northeastern New Mexico basin and arch complex: New Mexico Geological Society, Guidebook 27, p. 141–152. https://doi.org/10.56577/FFC-27.141

Rudolph, K., 2023, The Ancestral Rocky Mountain orogeny and evolution of the Permian Basin: New Mexico Geological Society, Guidebook 73, p. 147–164.

Rudolph, K., Leary, R., Smith, T., and Zellman, K., 2025, Evaluating Laramide orogenesis via flexural basin response in the San Juan Basin, New Mexico and Colorado: New Mexico Geological Society, Guidebook 75, p. 137–151. https://doi.org/10.56577/FFC-75.137

Saylor, J.E., Jordan, J.C., Sundell, K.E., Wang, X., Wang, S., and Deng, T., 2017, Topographic growth of the Jishi Shan and its impact on basin and hydrology evolution, NE Tibetan Plateau: Basin Research, v. 30, 544–563. https://doi.org/10.1111/bre.12264

Saylor, J.E., Rudolph, K.W., Sundell, K.E., and van Wijk, J., 2020, Laramide orogenesis driven by Late Cretaceous weakening of the North American lithosphere: Journal of Geophysical Research: Solid Earth, v. 125, e2020JB019570. https://doi.org/10.1029/2020JB019570

Sloss, L.L., ed., 1988, Sedimentary Cover—North American Craton, U.S.: The Geology of North America: Boulder, Geological Society America, v. D-2, 506 p. https://doi.org/10.1130/DNAG-GNA-D2

Soegaard, K., 1990, Fan-delta and braid-delta systems in Pennsylvanian Sandia Formation, Taos trough, northern New Mexico: Depositional and tectonic implications: Geological Society of America Bulletin, v. 102, p. 1325–1343. https://doi.org/10.1130/0016-7606(1990)102<1325:FDABDS>2.3.CO;2

Soreghan, G.S., Keller, G.R., Gilbert, M.C., Chase, C.G., and Sweet, D.E., 2012, Load-induced subsidence of the Ancestral Rocky Mountains recorded by preservation of Permian landscapes: Geosphere, v. 8, no. 3, p. 654–668. https://doi.org/10.1130/GES00681.1

Soto-Kerans, G.M., Stockli, D.F., Janson, X., Lawton, T.F., and Covault, J.A., 2020, Orogen proximal sedimentation in the Permian foreland basin: Geosphere, v. 16, p. 567–593. https://doi .org /10.1130/GES02108.1

Stevens, C.H., Stone, P., and Miller, J.S., 2005, A new reconstruction of the Paleozoic continental margin of southwestern North America: Implications for the nature and timing of continental truncation and the possible role of the Mojave-Sonora megashear, *in* Anderson, T.H., Nourse, J.A., McKee, J.W., Steiner, M.B., eds., The Mojave-Sonora Megashear Hypothesis: Development, Assessment, and Alternatives: Geological Society of America Special Paper 393, p. 597–618. https://doi.org/10.1130/0-8137-2393-0.597

Sweet, D.E., Brotherton, J.L., Chowdhury, N.U.M.K., and Ramsey, C.E., 2021, Tectonic subsidence analysis of the Ancestral Rocky Mountains from the interior to the southern margin: Palaeogeography, Palaeoclimatology, Palaeoecology, v. 576, p. 1–16. https://doi.org/10.1016/j.palaeo.2021.110508

Tesauro, M., Kaban, M.K., Mooney, W.D., and Cloetingh, S.A.P.L., 2014, Density, temperature, and composition of the North American lithosphere—New insights from a joint analysis of seismic, gravity, and mineral physics data: 2. Thermal and compositional model of the upper mantle: Geochemistry, Geophysics, Geosystems, v. 15, no. 12, p. 4808–4830. https://doi.org/10.1002/2014GC005484

Texas Railroad Commission, 2026, Oil and Gas Imaged Records Query Menu: https://www.rrc.texas.gov/resource-center/research/research-queries/imaged-records/imaged-records-menu/ (accessed April 2026).

Utah Department of Natural Resources Division of Oil, Gas and Mining, 2026, Data explorer: https://dataexplorer.ogm.utah.gov/ (accessed April 2026).

Wahlman, 2019, Pennsylvanian and Lower Permian fusulinid biostratigraphy of the Permian Basin region, southwestern USA, *in* S. C. Ruppel, ed., Anatomy of the Paleozoic Basin: The Permian Basin, USA (vol. 1): University of Texas at Austin, Bureau of Economic Geology, Report of Investigations No. 285, p. 167–227. https://doi.org/10.23867/RI0285-1

Waite, L., Fan, M., Collins, D., Gehrels, G., and Stern, R.J., 2020, Detrital zircon provenance evidence for an early Permian longitudinal river flowing into the Midland Basin of west Texas: International Geology Review, v. 62, 1224–1244. https://doi.org/10.1080/00206814.2020.1756930

Warren, J.K., 2010, Evaporites through time: Tectonic, climatic and eustatic controls in marine and nonmarine deposits: Earth-Science Reviews, v. 98, p. 217–268. https://doi.org/10.1016/j.earscirev.2009.11.004

Woodward, L.A., 1987, Geology and mineral resources of Sierra Nacimiento and vicinity, New Mexico: New Mexico Bureau Of Mines and Mineral Resources, Memoir 42, 84 p., 1 map. https://doi.org/10.58799/M-42

Zhang, H., Mann, P., Bird, D.E., and Rudolph, K., 2021, Integration of regional gravity modeling, subsidence analysis, and source rock maturity data to understand the tectonic and hydrocarbon evolution of the Permian Basin, West Texas: Interpretation, v. 9, no. 1, p. T161–T181. https://doi.org/10.1190/INT-2020-0065.1

Supplementary data can be found at https://nmgs.nmt.edu/repository/index.cfml?rid=2026002



Looking south along the crest of the Sandia Mountains. The Sandia Peak Tramway station is on Pennsylvanian Gray Mesa Formation. The Great Unconformity marks the slope break between well-exposed cliffs of Sandia granite and poorly exposed sedimentary rocks of the Sandia and Gray Mesa Formation. The western profile of the Sandia Mountains exhibits a mid-level topographic bench along the range. In the distance are the Manzanita, Manzano, and Los Pinos Mountains, which collectively define the eastern flank of the Albuquerque Basin. Photograph courtesy of Celestyn Brożek.